Nonlinear dynamics in a high-gain amplifier: the dc SQUID

A. R. Bulsara[1], K. Wiesenfeld[2], and M. E. Inchiosa[1]

[1]Space and Naval Warfare Systems Center Code D364, San Diego, CA 92152-5000, USA
[2]School of Physics, Georgia Institute of Technology, Atlanta, GA 30332, USA
bulsara@spawar.navy.mil

Received 26 April 2000, accepted 27 June 2000

Abstract. We study the detection of very weak time-periodic magnetic signals via a double-junction (dc) Superconducting Quantum Interference Device (SQUID). The device, represented by two coupled nonlinear differential equations for the quantum mechanical junction phase differences, admits long-time static or oscillatory solutions, the transition between them being easily controlled by experimentally accessible parameters. Gain is maximal when the device is tuned to the onset of the oscillatory solutions; i.e., when the minima in the 2D potential function disappear. We concentrate on the SQUID dynamics near this critical point and compute the oscillation frequency via a center manifold reduction of the full 2D dynamics. Knowing this frequency permits its exploitation as a detection/classification tool in magnetic remote sensing applications.

Keywords: SQUID, running solutions, amplification
PACS: 05.45.-a, 02.50.Ey, 02.30.Hq

1 Introduction

Superconducting Quantum Interference Devices (SQUIDs) [1] hold out the most promise for use in a variety of sensitive magnetic remote sensing applications including magneto-telluric exploration, biomagnetic sensing, NQR scanning for explosives/drugs, and communications applications. They are the most sensitive detectors of magnetic fields; however, they are quite vulnerable to noise, which can arise from a variety of sources: environmental, thermal, or noise coupled in from the biasing and readout electronics. Operated in the conventional flux-locked mode wherein the device is kept locked to an operating point in the linear regime of its transfer characteristic via feedback electronics, a very small amount of noise is often sufficient to lose the operating point ... the so-called "slew-rate" problem. Recently, a series of experiments [2] and supporting calculations [3, 4] have demonstrated that operating the SQUID as a free-running nonlinear dynamic device can enhance the noise tolerance if nonlinear phenomena are carefully used to alleviate noise problems. The objective in this case is not necessarily an enhancement of the SQUID's sensitivity; rather, it could be an

effective lowering of the noise floor of the readout system, resulting in an increase in the entire system's performance as reflected by its SNR, signal detection probability, and dynamic range. The above-mentioned research has exploited the SQUID's nonlinear transfer characteristic (see [5] for an excellent overview) in an attempt to enhance the noise-tolerance of SQUIDs; however, we wish to point out at least one additional novel use of SQUIDs [6] in the still-developing field of fluctuation-enhanced transport.

Signal detection and amplification in the single-junction (rf) SQUID has been explored in detail [7, 8]. Here, we consider the dynamics of the dc SQUID, a superconducting loop broken by two Josephson Junctions (symmetrically placed for convenience). The dynamics of this device are well-known (see e.g. [1, 9]) and we digress only briefly to write down the relevant equations without derivation. The variables of interest are the Schrödinger phase differences $\delta_{1,2}$ associated with the two (assumed identical) junctions, in terms of which we can express the experimentally measureable circulating current I_s in the SQUID loop:

$$\beta\frac{I_s}{I_0} = \delta_1 - \delta_2 - 2\pi\frac{\Phi_e}{\Phi_0}, \tag{1}$$

where $\beta \equiv 2\pi L I_0/\Phi_0$ is the nonlinearity parameter, I_0 the junction critical current, L the loop inductance, and Φ_e an external applied magnetic flux, $\Phi_0 \equiv h/2e$ being the flux quantum. In the absence of noise and a target magnetic flux, we can use the RSJ model to write down equations for the currents in the two arms of the SQUID via a lumped circuit representation [1, 9]; when transformed via the Josephson relations $\dot{\delta}_i = 2eV_i/\hbar$ linking the voltage and the quantum phase difference across the junction i, these equations take the form,

$$\tau\dot{\delta}_1 = \frac{I_b}{2} - I_s - I_0\sin\delta_1, \quad \tau\dot{\delta}_2 = \frac{I_b}{2} + I_s - I_0\sin\delta_2, \tag{2}$$

where $\tau \equiv \hbar/2eR$, R being the normal state resistance of the junctions. The dc bias current I_b is applied symmetrically to the loop. Rescaling the time by τ/I_0, one can write the above in the form $\dot{\delta}_i = -\nabla_i U(\delta_1, \delta_2)$ with the 2D potential function defined as

$$U(\delta_1, \delta_2) = -\cos\delta_1 - \cos\delta_2 - J(\delta_1 + \delta_2) + \frac{1}{2\beta}(\delta_1 - \delta_2 - 2\pi\Phi_{\rm ex})^2, \tag{3}$$

where we introduce the dimensionless bias current $J \equiv I_b/2I_0$ and normalized applied flux $\Phi_{\rm ex} \equiv \Phi_e/\Phi_0$.

The 2D potential function (3) has interesting properties. First, note that the *externally adjustable* bias parameters $\Phi_{\rm ex}$ and J control the symmetry and well-depth, respectively. Adjusting these parameters leads to a transition from a regime characterized by a multistable potential and long-time static solutions for the phase angles, to one wherein pairs of minima and saddles have coalesced to yield a potential with points of inflection, followed by (upon further adjusting the bias parameters) a potential with no minima. This latter regime, in which (2) admits spontaneous oscillatory solutions, is often referred to as the "running regime".

To make the physics of the near-critical dynamics in the running regime clearer, we first give a brief overview of the long-time SQUID dynamics in the static regime,

in the absence of external signals and noise sources. The condition $\dot{\delta}_i = 0$ immediately leads to the pair of phase equations,

$$\begin{aligned} &\delta_1 - \delta_2 - \frac{2\pi\Phi_e}{\Phi_0} + \beta(\sin\delta_1 - J) = 0 \\ &\delta_1 - \delta_2 - \frac{2\pi\Phi_e}{\Phi_0} - \beta(\sin\delta_2 - J) = 0. \end{aligned} \tag{4}$$

In addition, the phase continuity relation,

$$\delta_2 - \delta_1 = 2\pi n - 2\pi\frac{\Phi}{\Phi_0}, \tag{5}$$

n being an integer, links the phases, and the loop total flux is related to the circulating current by $\Phi = \Phi_e + LI_s$. Adding and subtracting the set (4), we are then led immediately to the current conservation relations for the loop:

$$2J = \sin\delta_1 + \sin\delta_2, \quad 2I_s = I_0(\sin\delta_2 - \sin\delta_1). \tag{6}$$

Further, the I_s equation can be manipulated to yield a transcendental equation for the circulating current:

$$\frac{I_s}{I_0} = -\sin\left(\pi\Phi_{\rm ex} + \frac{\beta I_s}{2I_0}\right)\cos\left[\sin^{-1}\left(J + \frac{I_s}{I_0}\right) + \pi\Phi_{\rm ex} + \frac{\beta I_s}{2I_0}\right]. \tag{7}$$

Equation (7) may be solved numerically for the circulating current; the ensuing transfer characteristic (TC) is periodic in the applied flux $\Phi_{\rm ex}$ and possibly hysteretic, with the hysteresis loop width controlled by the bias current J. For $J = 0$ one obtains hysteresis for any nonlinearity β; for $0 < J \leq 1$, hysteresis occurs over some range of β. Hysteresis in the output TC may be linked to a multistable potential function U. However, in practice the SQUID is an extremely fast device (time-constant $\tau \approx 10^{-12}$ sec) so that the potential description is merely a mathematical convenience. The switching time between wells is fast enough that the device is almost an ideal two-state device, so that many realistic external noise sources (other than purely thermal noise) must be treated as being correlated (i.e. the noise bandwidth is smaller than the SQUID bandwidth τ^{-1}). In the superconducting regime the SQUID dynamics (2) may be reduced to a 1D form, in terms of the normalized flux variable $x \equiv \Phi/\Phi_0$ (using the I_b current conservation relation):

$$\tau_s\dot{x} = -x - \Phi_{\rm ex} - \frac{\beta}{2\pi}\sin(\pi x)\cos(Z), \tag{8}$$

where we set $\tau_s = \beta\tau/2I_0$ and $Z = \pi x + \sin^{-1}[J + (2\pi/\beta)(x - \Phi_{\rm ex})]$. Equating the right hand side of (8) to zero and solving (numerically) for the x vs. $\Phi_{\rm ex}$ TC yields a curve identical to that obtained from the transcendental form (7), after we express I_s in terms of x. Note that, in this regime, the potential (3) can readily be transformed into a single-variable potential $U(x)$, whose derivative yields (up to a multiplicative constant) the negative of the right hand side of (8), as expected. Note, finally, that for any set of SQUID and bias parameters (β, J, $\Phi_{\rm ex}$), the numbers and locations of the

potential minima can be obtained via the zeros of the J current conservation relation (6), with one of the angles eliminated as a variable via (4). The zeros can also be obtained by looking at the intersections of the curves $\delta_1(\delta_2)$ and $\delta_2(\delta_1)$, given by (4) and plotted on the same axes [10].

We reiterate that the formalism in this section, in particular the conservation relations (6), are valid strictly when the potential U admits of stable minima, i.e. $\dot{\delta}_i = 0$. It is clear that the externally applied bias current J can be increased beyond the limiting value $J = 1$ past which the conservation relations (6) break down. At this point the potential U is no longer multistable, and the long time solutions for the phase angles are not static ($\dot{\delta}_i \neq 0$). In this "voltage state", an additional (normal) ohmic current must be added to the J conservation relation for it to be satisfied. The critical point at which this occurs has been calculated [4] in terms of the applied bias current and flux. We now consider this operating regime in greater detail.

2 Oscillatory Solutions in the Running Regime

A numerical solution of the SQUID dynamics (2) for different bias parameters leads to a computation of the bias current vs. dc bias flux TC for fixed J. Figure 1 shows the TC, with the transition to non-hysteretic behavior clearly visible. Experiments [2] have shown that the device response, measured as an output signal-to-noise ratio (SNR) at the frequency of a weak applied sinusoidal signal, is maximal in the transition regime from static to oscillatory (or running) solutions. This behavior is also evident in theoretically computed [4] SNR response curves, in the presence of a noise floor, shown in Fig. 1. From a computational standpoint, it is certainly more convenient to work in the non-hysteretic regime wherein the output variable (in this case, the circulating current I_s) is single-valued in the input. Then, one simply constructs the TC [11] and applies the signal and noise to the input [4]. In the hysteretic regime, on the other hand, one must integrate the coupled equations (2) and compute power spectra by averaging time series; this can prove cumbersome in some cases, and is certainly dependent on computing power.

The details of computation of the output SNR (shown in Fig. 1) will not be reproduced here [4]. We find remarkably good agreement with the experimental results; it is particularly gratifying to be able to "tune" the SQUID (i.e. adjust the TC) to yield optimal performance via adjustments of J and $\Phi_{\rm ex}$, since the third parameter β cannot be easily changed after fabrication.

2.1 Spontaneous Oscillation Frequency, Near the Singular Point

We now turn our attention to a discussion of the voltage regime, specifically the nature of the solutions to the dynamics (2) in this regime. Other researchers [12] have investigated the oscillatory regime via a computation of the voltage across the Josephson junctions; the Josephson relations relate this voltage (which can be experimentally measured) to the frequency of the oscillations. In our work [2,4], however, we consider the screening current I_s (replaced by its time-average in the oscillatory regime [11]) as the variable of interest.

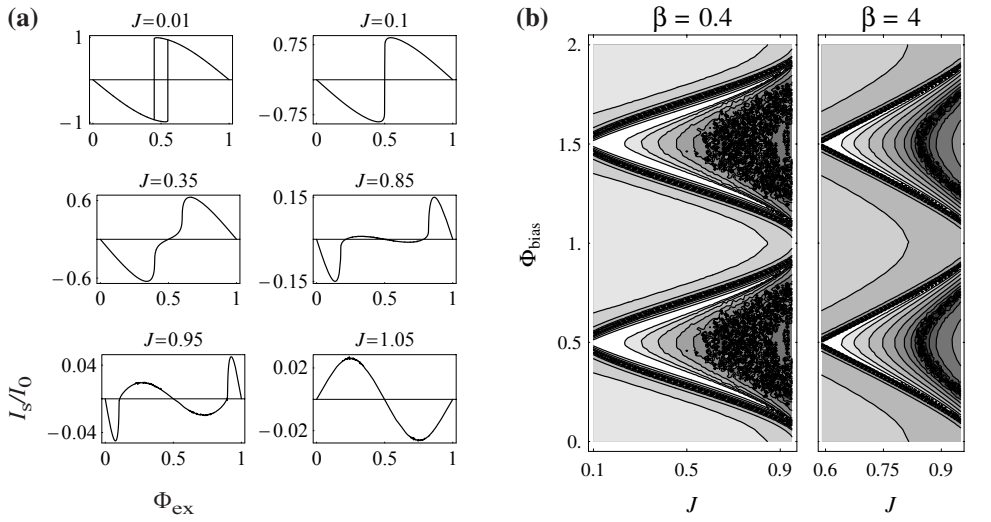

Fig. 1 (a) Transfer characteristic: time-averaged circulating current (see text) I_s/I_0 vs. applied flux $\Phi_{\rm ex}$ for $\beta = 0.4$. (b) Contour plot showing theoretically predicted output SNR (taken at target signal frequency), in the oscillatory solutions regime, vs. bias parameters $\Phi_{\rm bias}$ and J. SNR scale (black-to-white) corresponds to -28 dB to 32 dB, with contour lines spaced 5 dB apart. SNR values of -28 dB or less are represented by black; a "speckled" appearance in the black regions of the $\beta = 0.4$ plot is due to limited numerical precision. (After Ref. [4].)

The voltage regime is characterized by an imbalance in the current conservation relations (6) — the bias current I_b is no longer supported by the junction supercurrents and an ohmic current flows through the loop. The critical point at which this occurs is a saddle-node bifurcation characterized by the appearance of points of inflection in the potential function U. Past this critical point, the solutions for the phase angles δ_i are oscillatory [9,12], with the oscillation frequency typically being extremely high; this leads one to measure the time-averaged circulating current in experiments. The oscillations have zero frequency at the critical point and are typically nonsinusoidal, having the form of relaxation oscillations; this is readily apparent when one visualizes the system as a particle rolling down the potential walls. As each point of inflection is encountered, the particle undergoes a deceleration, followed by acceleration down the ensuing potential wall, until it arrives at the next "bottleneck". As the SQUID is biased farther into the running regime, the points of inflection give way to ramps (the curvature increases at the point of inflection), and the particle velocity through the bottleneck increases, even though it still undergoes a slowing down there. Hence, the oscillations become increasingly sinusoidal as we get deeper into the running regime. Our recent experiments and computations [2,4] show that the best response to an input signal (in the presence of a background noise floor) is obtained just past the bifurcation point, where one observes a very sensitive dependence of the solutions on the input: the high gain regime. Although various aspects of the oscillations have been analysed [12],

it is of interest to compute the frequency of the oscillations and the frequency scaling in terms of the control parameter "distance" from the singular point. Quantifying small changes in the frequency that occur in the presence of external (target) signals could afford a detection mechanism, and experiments involving synchronization to an external signal or to another SQUID would inevitably benefit from an *a priori* knowledge of the oscillation frequency in terms of the bias parameters.

Our calculation is made possible by the fact that close to the singular point there is a well-defined separation of time-scales that permits a center manifold reduction of the effective phase space. This renders the dynamics accessible to analytic computation close to the onset of the bifurcation. We start with the dynamics (2) in the absence of signals and noise, re-written in terms of the sum and difference variables $\Sigma \equiv (\delta_1 + \delta_2)/2, \delta \equiv (\delta_1 - \delta_2)/2$, with the result (letting $a \equiv \pi\Phi_{\rm ex}$),

$$\begin{aligned} \dot{\delta} &= -\frac{2}{\beta}(\delta - a) - \cos\Sigma \sin\delta \\ \dot{\Sigma} &= J - \cos\delta \sin\Sigma. \end{aligned} \tag{9}$$

We assume the dc flux bias a to be fixed at some nonzero value and let J_c be the critical value of J; at this value, the dynamics (9) are poised on the brink of the bifurcation, and the left hand side can be set equal to zero to solve for the critical values (Σ_0, δ_0). We then Taylor expand around these fixed points: $\delta = \delta_0 + x, \Sigma = \Sigma_0 + y$, with $|x|, |y| \ll 1$. To quadratic order,

$$\begin{aligned} \dot{x} &= -\left(\frac{2}{\beta} + A\right) x + By + Cx^2 + 2Dxy + Cy^2 + O(3) \\ \dot{y} &= -Ay + Bx + Dy^2 + 2Cxy + Dx^2 + O(3), \end{aligned} \tag{10}$$

where $A = \cos\Sigma_0 \cos\delta_0$, $B = \sin\delta_0 \sin\Sigma_0$, $C = \frac{1}{2}\sin\delta_0 \cos\Sigma_0$, and $D = \frac{1}{2}\cos\delta_0 \sin\Sigma_0$, and $O(3)$ represents terms of cubic order and smaller. At the bifurcation point, there is one non-vanishing eigenvalue λ of the linear portion of the dynamics. Introducing the transformation $\mathbf{S}$ that diagonalizes the linear part $\mathbf{DF}$ we have

$$\mathbf{S}\begin{pmatrix} x \\ y \end{pmatrix} = \begin{pmatrix} u \\ v \end{pmatrix}; \quad \mathbf{S} = \begin{pmatrix} \cos\theta & \sin\theta \\ -\sin\theta & \cos\theta \end{pmatrix} \tag{11}$$

and

$$\mathbf{S}\ \mathbf{DF}\ \mathbf{S}^{-1} = \begin{pmatrix} \lambda & 0 \\ 0 & 0 \end{pmatrix}; \quad \mathbf{DF} \equiv \begin{pmatrix} -2\beta^{-1} - A & B \\ B & A \end{pmatrix}, \tag{12}$$

where $\lambda = -2/\beta - 2\cos\Sigma_0 \cos\delta_0$, which must be negative so that the system orbits are attracted to the subspace $u = 0$ on the faster (order one) timescale λ^{-1}. In the diagonal representation we then have,

$$\frac{\mathrm{d}}{\mathrm{d}t}\begin{pmatrix} u \\ v \end{pmatrix} = \begin{pmatrix} \lambda & 0 \\ 0 & 0 \end{pmatrix}\begin{pmatrix} u \\ v \end{pmatrix} + \mathbf{S}\begin{pmatrix} Cx^2 + 2Dxy + Cy^2 \\ Dy^2 + 2Cxy + Dx^2 \end{pmatrix}. \tag{13}$$

The preceding steps may be repeated close to the bifurcation point ($J - J_c$ small), with an expansion about $(\delta_0, \Sigma_0, J_c)$; the resulting dynamics expanded to $O(2)$ is,

$$\frac{\mathrm{d}}{\mathrm{d}t}\begin{pmatrix} u \\ v \end{pmatrix} = \mathbf{S}\begin{pmatrix} 0 \\ J - J_c \end{pmatrix} + \begin{pmatrix} \lambda & 0 \\ 0 & 0 \end{pmatrix}\begin{pmatrix} u \\ v \end{pmatrix} + \mathbf{S}\begin{pmatrix} Cx^2 + 2Dxy + Cy^2 \\ Dy^2 + 2Cxy + Dx^2 \end{pmatrix}, \tag{14}$$

where $J - J_c$ is $O(2)$. It follows that $\dot{u} = \lambda u + O(2)$, so that the attracting subspace is $u = O(2)$, and the evolution of v on the center manifold is given by

$$\dot{v} = (J - J_c)\cos\theta + \alpha v^2 + O(3), \tag{15}$$

where it remains to determine the constant α. This is accomplished by explicitly computing the matrix product $\mathbf{S\,DF\,S}^{-1}$. After some calculations we obtain a product matrix having equal off-diagonal elements given by $(\cos\theta)\ [\sin\delta_0 \sin\Sigma_0 \cos\theta - \cos\Sigma_0 \cos\delta_0 \sin\theta] - (\sin\theta)\ [\sin\delta_0 \sin\Sigma_0 \sin\theta - (2\beta^{-1} + \cos\Sigma_0 \cos\delta_0)\cos\theta]$. The off-diagonal elements must vanish, so that we get after some manipulations:

$$\tan 2\theta = -\beta \sin\delta_0 \sin\Sigma_0, \tag{16}$$

which specifies the transformation matrix $\mathbf{S}$. We then explicitly carry out the transformation to the $(u - v)$ representation (14), with (x, y) expressed in terms of (u, v) by the inverse transformation:

$$\begin{pmatrix} x \\ y \end{pmatrix} = \mathbf{S}^{-1} \begin{pmatrix} u \\ v \end{pmatrix} = \begin{pmatrix} \cos\theta & -\sin\theta \\ \sin\theta & \cos\theta \end{pmatrix} \begin{pmatrix} u \\ v \end{pmatrix}, \tag{17}$$

after which we substitute for (x, y) in the $O(2)$ part of (14). We can identify α:

$$\alpha = -\sin\theta\,(C - D\sin 2\theta) + \cos\theta(D - C\sin 2\theta)\,,$$

which completes the normal form (15).

We are now in a position to integrate the normal form (15) analytically; this represents the dominant part (i.e. the passage through the "bottleneck" where the acceleration is the smallest, as explained earlier) of the SQUID dynamics. The integration yields,

$$v(t) = \sqrt{\frac{F}{\alpha}} \tan\left(\sqrt{F\alpha}\,t\right), \quad F \equiv (J - J_c)\cos\theta, \tag{18}$$

whence the period T of the oscillations is readily written down as

$$T = \frac{\pi}{\sqrt{\alpha(J - J_c)\cos\theta}}. \tag{19}$$

Equation (19) conforms to the period scaling law that accompanies bifurcations of this type [13]. We reiterate that the oscillations are *not* sinusoidal near the critical point, but approach sinusoidal behavior deep in the running regime; when $\Phi_{\rm ex} = 0.5$, the oscillations become most closely sinusoidal, and the average circulating current vanishes (Fig. 1a). We note, also, that the dc bias flux $\Phi_{\rm ex}$ could easily have been used as the control parameter (for constant bias current J) with an analogous scaling law for the spontaneous oscillations. In fact, in laboratory settings and practical applications, the device can be biased either via the current or flux input, with engineering considerations (e.g. impedance matching constraints that depend strongly on the input frequency) often determining which method is preferred. In all cases, the non-sinusoidal nature of the oscillations near the critical point can have some interesting consequences; we now provide a brief overview of some of this behavior.

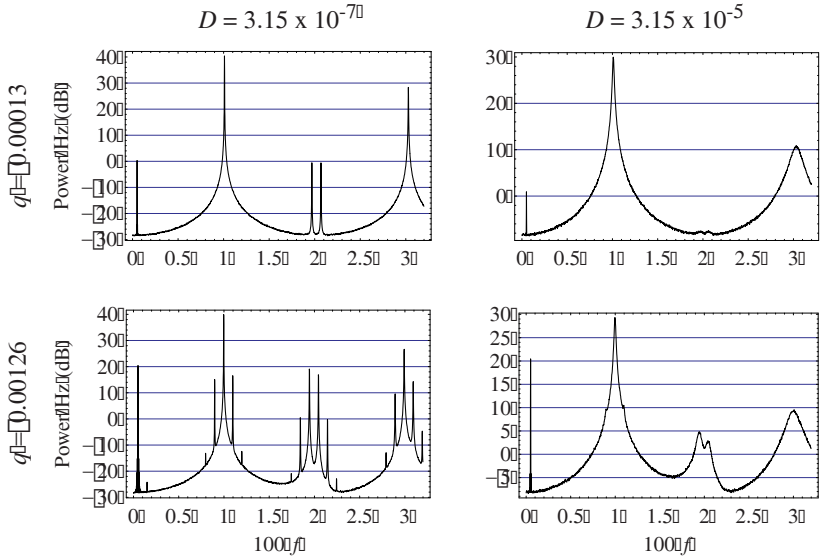

Fig. 2 Output PSD for external flux-bias (visible as sharp peak on extreme left of PSD) at low frequency. Flux amplitude $q = 0.00013$ (row 1), and 0.00126 (row 2). Noise intensity $2D$ (see text): 6.3×10^{-7} (column 1), and 6.3×10^{-5} (column 2). $\Phi_{\rm ex} = 0.5$. Broad peaks correspond to harmonics of the intrinsic oscillation frequency. Combination tones arising through nonlinear mixing of external and running frequencies are clearly visible; increasing the noise broadens and suppresses the peaks (see text).

2.2 *Near the Critical Point in the Oscillatory Regime; a Sampling of Cooperative Behavior*

In the preceding subsection we have derived the period of the spontaneous oscillations in the SQUID response just past the saddle-node bifurcation. Clearly, this represents an intrinsic (deterministic) time-scale in the system. One might expect a plethora of cooperative (and noise-mediated) behavior when the SQUID is externally biased with periodic signals having frequencies at or near the spontaneous oscillation frequency. In fact, such behavior should be expected of all the systems that display the class of dynamics considered in this work; we now display two examples of such behavior.

First we note that when applying an external bias $q\sin(\omega_s t)$, we can inductively couple it into the loop with the dc bias flux $\Phi_{\rm ex}$, or we may apply it as a current added to the bias current J. We consider both these situations here; in addition, we assume that the two junctions generate white Gaussian (thermal) noise, taken to have the same intensity $2D$ for each junction, but uncorrelated, that enters the dynamics (9) as an additional term $\sqrt{2D}\xi_i(t)$ to the bias current I_b, where $\xi(t)$ is zero-mean Gaussian noise having an autocorrelation $\langle \xi_i(t)\xi_i(t')\rangle = \delta(t-t')$.

In Fig. 2 we compute the output power spectral density (the Fourier transform of the autocorrelation function of the circulating current I_s), via direct simulation of the original dynamics (9). The SQUID is biased at the dc flux value $\Phi_{\rm ex} = 0.5$

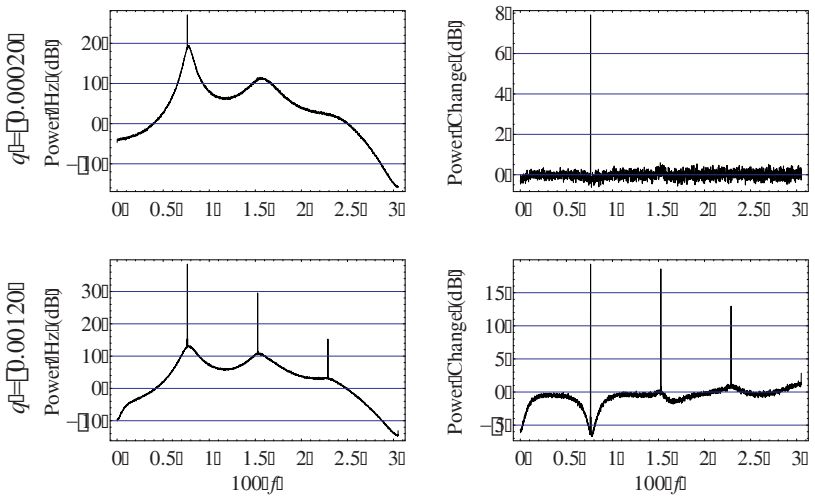

Fig. 3 Output PSD with external current bias at the running frequency $f = T^{-1}$. Signal amplitudes $q = 0.0002$ (row 1), and 0.0012 (row 2). Noise intensity 6.3×10^{-5}, $\Phi_{\rm ex} = 0.495$. Increasing the signal amplitude leads to lowering of noise background in the output around the running frequency as well as near dc; this is displayed in column 2 as a change in the output power relative to zero signal case.

corresponding to a symmetric transfer characteristic (see Fig. 1). Hence, the intrinsic oscillations produce (non-delta function) peaks at the odd harmonics of the fundamental frequency, in the absence of external signals. An external signal is flux-coupled into the device, producing peaks at the combination frequencies $|n\omega_s \pm 2\pi m/T|$. Increasing the external signal amplitude causes more of these combination tones to be visible above the noise background (see the first column in Fig. 2). Previous research [14] would indicate a stochastic resonance effect at every combination frequency, with the maximal response (quantified via an output SNR, for example) occurring at a different critical noise intensity for each frequency. While we do not consider this effect here, our results do indicate (column two) the effects of increasing the noise intensity. Note the dramatic lowering (even suppression) of all the peaks, as evidenced by the change in the vertical scales in column two (for the larger noise intensity).

The effect of applying an external signal via a current bias is shown in Fig. 3. As before, we include a noise source in our simulations of the coupled equations (9), and examine the output PSD for two signal amplitudes. The signal amplitudes are small enough that the dynamics of the noise-free system, while confined to a small region near the critical point, are not allowed to cross over into the running regime (to the left of the bifurcation point in Fig. 1), although the noise can cause occasional transitions with a transition probability that depends on its intensity. Once again, one observes broad peaks at the running solution frequency. However, with the signal frequency chosen to be the same as the running frequency, one obtains phase locking of the internal oscillations to the signal; the locking is characterized by the appearance

of sharp lines superimposed on the broad peaks, with a concommittant *lowering* of the noise floor near dc and the running frequency (second column in Fig. 3). Analogous effects are observed when the signal is injected at some detuned (with respect to T^{-1}) frequency, and also when it is injected as a flux, rather than a bias current. This noise-quenching, which is particularly pronounced at low frequencies, is a generic feature of nonlinear systems which undergo a frequency locking transition [15]. We are now studying this effect as a possible practical means of reducing the background noise in nonlinear devices that admit intrinsic oscillations. An *a priori* knowledge of the intrinsic oscillation frequency (19) is quite beneficial when optimizing these devices for specific operations.

We warmly thank Peter Hänggi for valuable (and voluble!) discussions on these and many other topics over the years. We also gratefully acknowledge support from the US Office of Naval Research, Physics Division.

References

[1] For good overviews see A. Barone, G. Paterno, *Physics and Applications of the Josephson Effect*, Wiley, New York 1982; J. Clarke, in *The new Superconducting Electronics* edited by H. Weinstock and R. Ralston, Kluwer, Amsterdam 1993
[2] A. Hibbs, in *Applied Nonlinear Dynamics and Stochastic Systems Near the Millenium*, AIP conference proceedings 411, edited by J. Kadtke and A. Bulsara, AIP Press, New York 1997; A. Hibbs and B. Whitecotton, Appl. Supercond. **6** (1999) 495
[3] M. Inchiosa, A. Bulsara, A. Hibbs, and B. Whitecotton, Phys. Rev. Lett. **80** (1998) 1381
[4] M. Inchiosa, A. Bulsara, K. Wiesenfeld, and L. Gammaitoni, Phys. Lett. A **252** (1999) 20; M. Inchiosa and A. Bulsara, in *Stochastic and Chaotic Dynamics in the Lakes* edited by D. S. Broomhead, E. Luchinskaya, P. V. E. McClintock, and T. Mullin, AIP, Melville 2000
[5] L. Gammaitoni, P. Hänggi, P. Jung, and F. Marchesoni, Rev. Mod. Phys. **70** (1998) 1
[6] I. Zapata, R. Bartussek, F. Sols, and P. Hänggi, Phys. Rev. Lett. **77** (1996) 2292
[7] A. Hibbs, A. Singsaas, E. Jacobs, A. Bulsara, J. Bekkedahl, and F. Moss, J. Appl. Phys. **77** (1995) 2582; R. Rouse, S. Han, and J. Lukens, Appl. Phys. Lett. **66** (1995) 108
[8] A. Bulsara, M. Inchiosa, and L. Gammaitoni, Phys. Rev. Lett. **77** (1996) 2162; M. Inchiosa, A. Bulsara, and L. Gammaitoni, Phys. Rev. E **55** (1997) 4049; M. E. Inchiosa and A. R. Bulsara, Phys. Rev. E **58** (1998) 115
[9] H. Koch, in *Sensors, A Comprehensive Survey Vol. 5* edited by W. Gopel, J. Hesse, and J. Zemel, VCH, New York 1989
[10] C. Tesche, J. Low Temp. Phys. **44** (1981) 119
[11] In experiments [2], only the time-averaged circulating current $\bar{I}_s$ is measureable because of the extremely high frequency (predicated by the time-constant τ) of the spontaneous oscillations in the running state. The TC is then simply a plot of $\bar{I}_s$ vs. Φ_{ex} for a given J.
[12] E. Ben-Jacob and Y. Imry, J. Appl. Phys. **52** (1981) 6806; P. Carelli and G. Paterno, in *Principles and Applications of Superconducting Quantum Interference Devices* edited by A. Barone, World Scientific, Singapore 1992
[13] See e.g. S. Strogatz, *Nonlinear Dynamics and Chaos*, Perseus Press, New York 1994
[14] A. Bulsara, M. Inchiosa, and L. Gammaitoni, Phys. Rev. Lett. **77** (1996) 2162; M. Inchiosa, A. Bulsara, and L. Gammaitoni, Phys. Rev. E **55** (1997) 4049; A. Grigorienko, P. Nikitin, and V. Roshchepkin, Sov. Phys. JETP **85** (1997) 343
[15] K. Wiesenfeld and I. Satija, Phys. Rev. B **36** (1987) 2483